# Numerical Study of Performance of Porous Fin Heat Sink of Functionally Graded Material for Improved Thermal Management of Consumer Electronics

George A. Oguntala, *Member, IEEE*, Gbeminiyi M. Sobamowo, Raed Abd-Alhameed, *Senior Member, IEEE* and James M. Noras

***Abstract*—The ever-increasing demand for high performance electronic and computer systems has unequivocally called for increased microprocessor performance. However, increasing microprocessor performance requires increasing the power and on-chip power density of the microprocessor, both of which are associated with increased heat dissipation. In recent times, thermal management of electronic systems has gained intense research attention due to increased miniaturization trend in the electronics industry. In the paper, we present a numerical study on the performance of a convective-radiative porous heat sink with functionally graded material for improved cooling of various consumer electronics. For the theoretical investigation, the thermal property of the functionally graded material is assumed as a linear and power-law function. We solved the developed thermal models using Chebyshev spectral collocation method. The effects of in-homogeneity index of FGM, convective and radiative parameters on the thermal behaviour of the porous heat sink are investigated. The present study shows that increase in the in-homogeneity index of FGM, convective and radiative parameter improves the thermal efficiency of the porous fin heat sink. The thermal predictions made in this study using Chebyshev spectral collocation method agrees excellently with the established results of Runge-Kutta with shooting and homotopy analytical method.**

***Index Terms*—Consumer electronics, functionally graded material, heatsink, porous fin, thermal management**

**SYMBOLS**

| | |
|---|---|
| $A_r$ | Fin base-to-surface aspect ratio |
| $A$ | Fin cross-sectional area |
| $A_b$ | Fin base cross-sectional area |
| $A_s$ | Porous fin surface area |
| $h$ | Coefficient of heat transfer |
| $h_b$ | Coefficient of heat transfer at base |
| $g$ | Gravity constant |
| $h$ | Heat transfer coefficient over the fin surface |
| $k$ | Thermal conductivity of FGM |
| $k_b$ | Thermal conductivity of FGM at the base of fin |
| $L$ | Fin length |
| $w$ | Fin width |
| $t$ | Fin thickness |
| $m$ | Mass flow rate of fluid passing through the porous fin |
| $P$ | Fin perimeter |
| $T$ | Fin temperature |
| $T_a$ | Ambient temperature |
| $T_b$ | Base temperature of fin |
| v | Average velocity of the fluid passing through the porous fin |
| $Q$ | Dimensionless heat transfer rate per unit area |
| $Q_b$ | Dimensionless heat transfer rate at porous fin base |
| $Q_s$ | Dimensionless heat transfer rate at solid fin base |
| $M$ | Dimensionless thermo-geometric parameter |
| $X$ | Dimensionless length of the fin |
| $H$ | Dimensionless heat transfer coefficient at the fin base |
| W | Width of the fin |
| $k_{eff}$ | Effective thermal conductivity ratio |
| $B_i$ | Biot number |
| $Da$ | Darcy number |
| $Ra$ | Rayleigh number |
| $S_h$ | Porosity parameter |

**Greek Symbols**

| | |
|---|---|
| β | in-homogeneity index |
| δ | fin thickness |
| $\delta_b$ | fin base thickness |
| θ | Dimensionless temperature |
| $\theta_b$ | Dimensionless temperature at fin base |
| γ | Dimensionless internal heat generation parameter |
| η | Efficiency of the fin |
| β' | Coefficient of thermal expansivity |
| ε | Emissivity |
| φ | Porosity |
| υ | Kinematic viscosity |
| ρ | Density of single-phase fluid |

Manuscript received on 3rd October 2017, revised 5th March 2019. This work was supported in part from the PhD sponsorship of the first author by the Tertiary Education Trust Fund of the Federal Government of Nigeria.

G. A. Oguntala, R. A. Abd-Alhameed and J.M. Noras are with the Department of Biomedical and Electronics Engineering, Faculty of Engineering and Informatics, University of Bradford, West Yorkshire, BD7 1DP, UK (e-mail: g.a.oguntala@bradford.ac.uk; r.a.a.abd@bradford.ac.uk; j.m.noras@bradford.ac.uk)

G. M. Sobamowo is with the Department of Mechanical Engineering, Faculty of Engineering, University of Lagos, Akoka, 100213, Lagos, Nigeria (e-mail: gsobamowo@unilag.edu.ng).

## I. Introduction

THE past few decades have witnessed a revolutionary increase in the semiconductor industry resulting in the development of high computing electronic systems. This evolution has consequently witnessed a huge demand for high-performance consumer electronics. One key component in the middle of this evolutionary development is the microprocessor. Following Moore's law [1], recent

microprocessors are designed with doubled transistor density every two years to achieve increased performance and increased on-chip power density with each new technology generation [2]. Moreover, recent computer and electronic systems are designed to tradeoff size with efficiency to achieve miniaturized packaging. One key consequence of such design requirement is the building of excess heat within the thermal components and especially from the microprocessor of these systems. As a result, the ineffective removal of excess heat from electronic components would result in adverse effect on the overall functionality and eventual damage to the circuitry of the electronic device. In recent times, such a situation has led to huge product recall from several manufacturers. Consequently, the pursuit of miniaturized packaging and optimum heat dissipation of electronic components and systems is ever-increasing. Reliable cooling technology or thermal management of key electronic components such as chip has been one key design goal in the modern advanced semiconductor industry. This makes the subject of thermal management of electronic system an interesting research area.

Heatsink are heat exchangers used to dissipate heat from functional electronic components into their operating environments. This allows the working temperature of electronic device to operate below their respective allowable maximum temperature usually ranging between 70$^{o}$C and 120$^{o}$C. However, one key approach to achieve miniaturized and thermally-reliable electronic systems is to enhance their thermal performance via increased heat transfer between the device surface and its surrounding environment using extended surface or fin. A few commercially-available heatsinks with longitudinal fins is shown in Fig. 1.

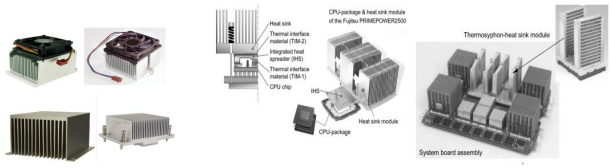


Fig. 1. Commercial heat sinks with longitudinal plate fins [3]

Fins are extended surfaces used to enhance heat dissipation from the thermal surface of electronic components through natural convection, normally with air as the cooling medium for electronic cooling. Improved heat dissipation using porous fin gained its popularity following the work of [4]. With improved performance over solid fins of equal dimension and weight, the porous fin has been identified as a viable candidate for thermal enhancement of electronic systems. Consequently, the subject of fin performance for improved cooling of electronic components as a means to ameliorate the issue of excess heat dissipation and achieve thermally-efficient, miniaturized high-performance electronic systems is rapidly gaining research momentum.

Numerous works have been carried out in the literature to investigate the thermal behaviour of fins for improved cooling. Some of these works performed different analysis on heat transfer enhancement in miniature, micro, microchannel and micro-pin-fin heatsinks using nanofluid [5-11]. Other studies focus on the effects of various convective parameters including channel cross-sectional geometry, properties of convectional airflow, effects of particulates, features of channel cross-section, variable geometries and air flow paths on the fin performance for effective cooling. Most of these works employ various experimental, analytical and numerical methodologies to propose effective cooling approaches of various electronic systems [12-18]. The developed models are used to investigate the various characteristics of heat transfer, pressure drop, and fluid flow to achieve improved cooling via heatsink.

Recent research identifies materials of changing composition, microstructure, or porosity across the material volume as a viable candidate to improve the thermal performance of heat sinks [19, 20]. Such inhomogeneous material where the physical properties including electrical, magnetic, mechanical, thermal and chemical vary along the specific axis is generally regarded as functionally graded material (FGM). It is noteworthy that some research identifies phase-change materials as reliable heatsink fin material for passive cooling of thermal components [21-23]. Nevertheless, the variation in the properties of FGM along any specific axis is based on porosity and pore-size-gradient structure, chemical-gradient structure and microstructural-gradient structure. However, FGM, though initially applied as high-temperature structure material due to its high thermal stress behaviour gained its popularity due to its diverse applications areas including nuclear, automotive, aerospace and optoelectronics. Nonetheless, an in-depth review of previous works shows the ability of heat enhancement of porous media and FGM in thermal systems.

Therefore, the objective of the present investigation is to understand the thermal capability of FGM as heatsink fin material for efficient cooling of various consumer and high power electronics. To achieve our research objective, a thermal characterization of heat transfer enhancement of convective-radiative porous fin of FGM using Chebyshev spectral collocation method (CSCM) is carried out. CSCM is applied in the present paper due to its well-established fast rate of convergence, suitability, and high-level of accuracy over most established numerical methods in the field of numerical simulations [24-28]. The thermal property of the FGM is assumed as a linear and power-law function [29, 30]. The numerical solution obtained in the study is used to perform parametric studies on the effects of in-homogeneity index of FGM, convective and radiative variables on the thermal performance of the porous heatsink with FGM. The result obtained from the present study is compared with the established result of numerical and approximate analytical studies and excellent agreement is established.

The rest of the paper is organized as follows: Section II presents the formulation of the fin problem. In Section IV, we discussed the analysis of the porous fin heatsink with FGM using CSCM, whilst we extensively present the results of our investigation in Section V. We conclude the study in Section VI.

## II. FORMULATION OF THE FIN PROBLEM

In this section, we formulate the fin problem. A porous fin heatsink made of FGM under a convective-radiative condition

is considered. The porous fin has the following parameters: length *L*, thickness *t* exposed on both faces and is operating at a temperature $T_\infty$ as shown in Fig. 2.

To model the problem, the following assumptions are made.

i. The porous medium is homogeneous, isotropic and saturated with a single-phase fluid.
ii. Physical properties of solid as well as the fluid of porous medium are regarded as constant except density variation of the liquid, which might affect the buoyancy term where Boussinesq approximation is employed.
iii. Porous medium and fluid are locally in thermodynamic equilibrium.
iv. Temperature profile within the fin is 1-dimensional, as temperature varies along the length only but is time invariant.
v. No thermal contact resistance exists at the base of the fin and fin tip, as it is of adiabatic type.

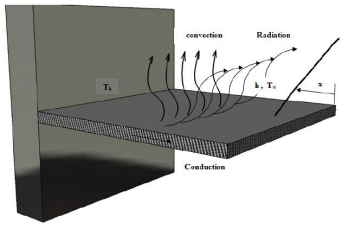


Fig. 2. Schematic representation of the adopted convective-radiative fin used in the study [31]

Using Darcy's law, the energy balance based on the above model assumptions expressed in the form:

$$q_x = \left(q_x + \frac{dq}{dx}dx\right) = \dot{m}c_p\left(T - T_a\right) + hP\left(1-\tilde{\varepsilon}\right)\left(T - T_a\right)dx + \sigma\varepsilon P\left(T^4 - T_a^4\right) \tag{1}$$

where $\dot{m}$ is the rate of flow of fluid through the porous medium and is expressed as:

$$\dot{m} = \rho u(x) W \partial x \tag{2}$$

and

$$u(x) = \frac{gK\beta}{v}\left(T - T_a\right) \tag{3}$$

The expression in Eq. (1) becomes

$$q_x - \left(q_x + \frac{dq}{dx}dx\right) = \frac{\rho c_p gK\beta}{v}(T - T_a)^2 dx + hP(1-\varphi)(T - T_a)dx + \sigma\varepsilon P(T^4 - T_a^4)dx \tag{4}$$

However, as $\partial x \rightarrow 0$ , Eq. (4) becomes

$$-\frac{dq}{dx} = \frac{\rho c_p gK\beta}{v}(T - T_a)^2 + hP(1-\phi)\left(T - T_a\right) + \sigma\varepsilon P(T^4 - T_a^4) \tag{5}$$

Conduction in the porous fin of FGM is governed by Fourier's law and is expressed as:

$$q = -k_{eff}(x) A_{cr}\frac{dT}{dx} \tag{6}$$

where

$$k_{eff}(x) = \phi k_f + (1-\phi)k_s$$

Moreover, by applying Rosseland diffusion approximation [32], the radiated heat transfer rate is obtained as:

$$q = -\frac{4\sigma A_{cr}}{3\beta_R}\frac{\partial T^4}{\partial x} \tag{7}$$

Therefore, the total rate of heat transfer of the porous fin of FGM could be expressed as:

$$q = -k_{eff}(x) A_{cr}\frac{dT}{dx} - \frac{4\sigma A_{cr}}{3\beta_R}\frac{dT^4}{dx} \tag{8}$$

However, on substituting Eq. (8) in Eq. (5), we have

$$\frac{d}{dx}\left(k_{eff}(x) A_{cr}\frac{dT}{dx} + \frac{4\sigma A_{cr}}{3\beta_R}\frac{dT^4}{dx}\right) = \frac{\rho c_p gK\beta}{v}(T - T_a)^2 + hP(1-\varphi)(T - T_a) + \sigma\varepsilon P(T^4 - T_a^4) \tag{9}$$

By simplifying Eq. (9), we derive the governing differential equation of the porous fin with FGM as:

$$\frac{d}{dx}\left(k_{eff}(x)\frac{dT}{dx}\right) + \frac{4\sigma}{3\beta_R}\frac{d}{dx}\left(\frac{dT^4}{dx}\right) - \frac{\rho c_p gK\beta}{tv}\left(T - T_a\right)^2 - \frac{h(1-\varphi)}{t}\left(T - T_a\right) - \frac{\sigma\varepsilon}{t}\left(T^4 - T_a^4\right) = 0 \tag{10}$$

where the boundary conditions are:

$$x = 0, \quad \frac{dT}{dx} = 0$$
$$x = L, \quad T = T_b \tag{11}$$

It is noteworthy that the present work focuses on the thermal analysis of the FGM when the base temperature of the fin suddenly increases to a certain value $T_b$, and is kept constant thereafter, i.e. an operating condition where heat transfer coefficient at the base of the fin is high. However, several existing works investigate high and low heat flux to evaluate fin performance [33-36].

### *A. Consideration I – When temperature difference within the fin material during heat transfer is negligible*

If there exists a small temperature difference between the base and tip of the fin during the heat flow, the convective term which is a linear function of temperature dominates the heat flow process and under such a scenario, the term $T^4$ in the radiative term can also be expressed as a linear function of temperature [37, 38]. This is because the radiative heat transfer dominates heat flow with a relatively high-temperature difference. However, under the existence of small temperature difference within the fin, the use of temperature-invariant physical and thermal properties of the fin can be used without any loss in accuracy and generality. Therefore, under the present thermal scenario, the application of temperature-invariant physical and thermal properties of the fin is required and the term $T^4$ is expressed as a linear function of temperature as:

$$T^4 = T_\infty^4 + 4T_\infty^3\left(T - T_\infty\right) + 6T_\infty^2\left(T - T_\infty\right)^2 + \ldots.. \cong 4T_\infty^3 - 3T_\infty^4 \tag{12}$$

by substituting Eq. (12) in Eq. (10), we obtain Eq. 13

$$\frac{d}{dx}\left(k_{eff}(x)\frac{dT}{dx}\right) + \frac{16\sigma}{3\beta_R}\frac{\partial^2 T}{\partial x^2} - \frac{\rho c_p gK\beta}{tv}\left(T - T_a\right)^2 - \frac{h(1-\varphi)}{t}\left(T - T_a\right) - \frac{4\sigma\varepsilon PT_a^3}{t}\left(T - T_a\right) = 0 \tag{13}$$

The spatial-dependent thermal conductivity of the FGM fin is therefore expressed as:

Linear-law function

$$k_{eff}(x) = k_0\left[1+\beta\left(\frac{x}{L}\right)\right] \tag{14}$$

Power-law function

$$k_{eff} = k_0\left(\frac{x}{L}\right)^{-\beta} \tag{15}$$

We introduce the dimensionless parameters of Eq. (16) and substitute them into Eqs. (13) - (15)

$$X=\frac{x}{L},\ H=\frac{\sigma_m B_0^2 u^2}{k_{eff}A_b},\ C_T=\frac{T_\infty}{T_b-T_\infty},\ \theta=\frac{T-T_a}{T_b-T_a},\quad Rd=\frac{4\sigma T_\infty^3}{3\beta_R k_{eff}},$$
$$Ra=\frac{g\beta\left(T_b-T_\infty\right)b^3}{\alpha\nu},\ Nc^2=\frac{pbh(1-\varphi)}{A_b k_{eff}},\ Nr=\frac{4\sigma b T_\infty^3}{k_{eff}}, \tag{16}$$

Therefore, the dimensionless form of the governing equation can be expressed as:

Linear-law function

$$\frac{d}{dX}\left[(1+\beta X)\frac{d\theta}{dX}\right]+4Rd\frac{d^2\theta}{dX^2}-Ra\theta^2-Nc^2\theta-Nr\theta=0 \tag{17}$$

Power-law function

$$\frac{d}{dX}\left[\left(X^{-\beta}\right)\frac{d\theta}{dX}\right]+4Rd\frac{d^2\theta}{dX^2}-Ra\theta^2-Nc^2\theta-Nr\theta=0 \tag{18}$$

on expanding Eq. (17) and (18), we obtain

Linear-law function

$$\frac{d^2\theta}{dX^2}+\beta X\frac{d^2\theta}{dX^2}+\beta\frac{d\theta}{dX}+4Rd\frac{d^2\theta}{dX^2}-Ra\theta^2-Nc^2\theta-Nr\theta=0 \tag{19}$$

Power-law function

$$X^{-\beta}\frac{d^2\theta}{dX^2}-\beta X^{-\beta-1}\frac{d\theta}{dX}+4Rd\frac{d^2\theta}{dX^2}-Ra\theta^2-Nc^2\theta-Nr\theta=0 \tag{20}$$

and the dimensionless boundary conditions are:

$$X=0,\quad \frac{d\theta}{dX}=0$$
$$X=1,\quad \theta=1 \tag{21}$$

For the solid fin, i.e. non-porous fin with FGM, the governing differential equations are:

Linear-law function

$$\frac{d^2\theta}{dX^2}+\beta X\frac{d^2\theta}{dX^2}+\beta\frac{d\theta}{dX}+4Rd\frac{d^2\theta}{dX^2}-Nc^2\theta-Nr\theta=0 \tag{22}$$

Power-law function

$$X^{-\beta}\frac{d^2\theta}{dX^2}-\beta X^{-\beta-1}\frac{d\theta}{dX}+4Rd\frac{d^2\theta}{dX^2}-Nc^2\theta-Nr\theta=0 \tag{23}$$

Therefore, the approximate analytical solution is developed using the mean-value theorem as

Linear-law function

$$\theta(X)=\frac{\left\{\left\{\left(\frac{-\beta+\sqrt{\beta^2+4\left(Nc^2+Nr\right)\left(1+\frac{\beta}{2}\right)}}{2\left(1+\frac{\beta}{2}\right)}\right)\exp\left\{\left(\frac{-\beta+\sqrt{\beta^2+4\left(Nc^2+Nr\right)\left(1+\frac{\beta}{2}\right)}}{2\left(1+\frac{\beta}{2}\right)}\right)+\left(\frac{-\beta-\sqrt{\beta^2+4\left(Nc^2+Nr\right)\left(1+\frac{\beta}{2}\right)}}{2\left(1+\frac{\beta}{2}\right)}\right)(1-X)\right\}\right\}\right.}{\left.-\left\{\left(\frac{-\beta-\sqrt{\beta^2+4\left(Nc^2+Nr\right)\left(1+\frac{\beta}{2}\right)}}{2\left(1+\frac{\beta}{2}\right)}\right)\exp\left\{\left(\frac{-\beta-\sqrt{\beta^2+4\left(Nc^2+Nr\right)\left(1+\frac{\beta}{2}\right)}}{2\left(1+\frac{\beta}{2}\right)}\right)+\left(\frac{-\beta+\sqrt{\beta^2+4\left(Nc^2+Nr\right)\left(1+\frac{\beta}{2}\right)}}{2\left(1+\frac{\beta}{2}\right)}\right)(1-X)\right\}\right\}\right\}}$$
$$\left\{\left\{\left(\frac{-\beta+\sqrt{\beta^2+4\left(Nc^2+Nr\right)\left(1+\frac{\beta}{2}\right)}}{2\left(1+\frac{\beta}{2}\right)}\right)\exp\left\{\left(\frac{-\beta+\sqrt{\beta^2+4\left(Nc^2+Nr\right)\left(1+\frac{\beta}{2}\right)}}{2\left(1+\frac{\beta}{2}\right)}\right)\right\}\right\}-\left\{\left(\frac{-\beta-\sqrt{\beta^2+4\left(Nc^2+Nr\right)\left(1+\frac{\beta}{2}\right)}}{2\left(1+\frac{\beta}{2}\right)}\right)\exp\left\{\left(\frac{-\beta-\sqrt{\beta^2+4\left(Nc^2+Nr\right)\left(1+\frac{\beta}{2}\right)}}{2\left(1+\frac{\beta}{2}\right)}\right)\right\}\right\}\right\} \tag{24}$$

Power-law function

$$\theta(X)=\frac{\left\{\left\{\left(\frac{-\beta\left(\frac{1}{2}\right)^{-\beta-1}+\sqrt{\left[\beta\left(\frac{1}{2}\right)^{-\beta-1}\right]^2+4\left(Nc^2+Nr\right)\left(\frac{1}{2}\right)^{-\beta}}}{2\left(\frac{1}{2}\right)^{-\beta}}\right)\exp\left\{\left(\frac{-\beta\left(\frac{1}{2}\right)^{-\beta-1}+\sqrt{\left[\beta\left(\frac{1}{2}\right)^{-\beta-1}\right]^2+4\left(Nc^2+Nr\right)\left(\frac{1}{2}\right)^{-\beta}}}{2\left(\frac{1}{2}\right)^{-\beta}}\right)\right\}+\left(\frac{-\beta\left(\frac{1}{2}\right)^{-\beta-1}-\sqrt{\left[\beta\left(\frac{1}{2}\right)^{-\beta-1}\right]^2+4\left(Nc^2+Nr\right)\left(\frac{1}{2}\right)^{-\beta}}}{2\left(\frac{1}{2}\right)^{-\beta}}\right)(1-X)\right\}\right\}-\left\{\left\{\left(\frac{-\beta\left(\frac{1}{2}\right)^{-\beta-1}-\sqrt{\left[\beta\left(\frac{1}{2}\right)^{-\beta-1}\right]^2+4\left(Nc^2+Nr\right)\left(\frac{1}{2}\right)^{-\beta}}}{2\left(\frac{1}{2}\right)^{-\beta}}\right)\exp\left\{\left(\frac{-\beta\left(\frac{1}{2}\right)^{-\beta-1}-\sqrt{\left[\beta\left(\frac{1}{2}\right)^{-\beta-1}\right]^2+4\left(Nc^2+Nr\right)\left(\frac{1}{2}\right)^{-\beta}}}{2\left(\frac{1}{2}\right)^{-\beta}}\right)\right\}+\left(\frac{-\beta\left(\frac{1}{2}\right)^{-\beta-1}+\sqrt{\left[\beta\left(\frac{1}{2}\right)^{-\beta-1}\right]^2+4\left(Nc^2+Nr\right)\left(\frac{1}{2}\right)^{-\beta}}}{2\left(\frac{1}{2}\right)^{-\beta}}\right)(1-X)\right\}\right\}}{\left\{\left\{\left(\frac{-\beta\left(\frac{1}{2}\right)^{-\beta-1}+\sqrt{\left[\beta\left(\frac{1}{2}\right)^{-\beta-1}\right]^2+4\left(Nc^2+Nr\right)\left(\frac{1}{2}\right)^{-\beta}}}{2\left(\frac{1}{2}\right)^{-\beta}}\right)\exp\left\{\left(\frac{-\beta\left(\frac{1}{2}\right)^{-\beta-1}+\sqrt{\left[\beta\left(\frac{1}{2}\right)^{-\beta-1}\right]^2+4\left(Nc^2+Nr\right)\left(\frac{1}{2}\right)^{-\beta}}}{2\left(\frac{1}{2}\right)^{-\beta}}\right)\right\}\right\}-\left\{\left\{\left(\frac{-\beta\left(\frac{1}{2}\right)^{-\beta-1}-\sqrt{\left[\beta\left(\frac{1}{2}\right)^{-\beta-1}\right]^2+4\left(Nc^2+Nr\right)\left(\frac{1}{2}\right)^{-\beta}}}{2\left(\frac{1}{2}\right)^{-\beta}}\right)\exp\left\{\left(\frac{-\beta\left(\frac{1}{2}\right)^{-\beta-1}-\sqrt{\left[\beta\left(\frac{1}{2}\right)^{-\beta-1}\right]^2+4\left(Nc^2+Nr\right)\left(\frac{1}{2}\right)^{-\beta}}}{2\left(\frac{1}{2}\right)^{-\beta}}\right)\right\}\right\}} \tag{25}$$

### *B. Consideration II – When temperature difference within the fin material during heat transfer is high*

In this case scenario, we consider a condition where the temperature difference within the fin material is high. Under this condition, the physical and thermal properties of the fin are temperature-dependent and $T^4$ cannot be linearized as a function of temperature. Therefore, we substitute the dimensionless parameters in Eq. (10) to obtain the linear and power functions as:

Linear-law function

$$\frac{d^2\theta}{dX^2}+\beta X\frac{d^2\theta}{dX^2}+\beta\frac{d\theta}{dX}+4Rd\frac{d^2\theta}{dX^2}-Ra\theta^2-Nc^2\theta-Nr\left[\left(\theta+C_T\right)^4-C_T^4\right]=0 \tag{26}$$

Power-law function

$$X^{-\beta}\frac{d^2\theta}{dX^2}-\beta X^{-\beta-1}\frac{d\theta}{dX}+4Rd\frac{d^2\theta}{dX^2}-Ra\theta^2-Nc^2\theta-Nr\left[\left(\theta+C_T\right)^4-C_T^4\right]=0 \tag{27}$$

However, by expanding the radiative term of Eq. (26) and (27) for simplification, we obtain:

Linear-law function

$$\frac{d^2\theta}{dX^2}+\beta X\frac{d^2\theta}{dX^2}+\beta\frac{d\theta}{dX}+4Rd\frac{d^2\theta}{dX^2}-Ra\theta^2-Nc^2\theta-Nr\theta^4-4NrC_T\theta^3$$
$$-6NrC_T^2\theta^2-4NrC_T^3\theta=0 \tag{28}$$

Power-law function

$$X^{-\beta}\frac{d^2\theta}{dX^2}-\beta X^{-\beta-1}\frac{d\theta}{dX}+4Rd\frac{d^2\theta}{dX^2}-Ra\theta^2-Nc^2\theta-Nr\theta^4-4NrC_T\theta^3$$
$$-6NrC_T^2\theta^2-4NrC_T^3\theta=0 \tag{29}$$

## III. METHOD OF ANALYSIS OF POROUS FIN HEATSINK WITH FGM USING CSCM

This section covers the solution of the developed fin model. We apply CSCM to obtain the closed-form solution of Eq. (28) and (29). To apply CSCM, an expansion of the parameters is made at collocation points, whilst the derivative of the parameters at each collocation points is derived. Thereafter, we convert the expanded parameters into differential equations, before seeking the approximate solution in physical space. However, by seeking for the approximate solution, which is a global Chebyshev polynomial of degree $N$ defined on the interval [-1, 1], we discretized the interval using collocation points to define the Chebyshev nodes in [-1, 1] as:

$$x_j=\cos\left(\frac{j\pi}{N}\right),\quad \text{where } j=0,1,2,.....N \tag{30}$$

We define the derivative of both functions at the collocation points as:

$$f^n\left(x_j\right)=\sum_{j=0}^{N}d_{kj}^n f\left(x_j\right),\quad n=1,2. \tag{31}$$

where $d_{kj}^n$ is the differential matrix of order $n$ and is expressed as:

$$d_{kj}^1=\frac{4\gamma_j}{N}\sum_{n=0,l=0}^{N}\sum_{n+l=odd}^{N-1}\frac{n\gamma_n}{c_l}T_l^n\left(x_k\right)T_n\left(x_j\right), \tag{32}$$

where $k, j=0,1,...N$

and

$$d_{kj}^2=\frac{2\gamma_j}{N}\sum_{n=0,l=0}^{N}\sum_{n+l=even}^{N-1}\frac{n\gamma_n\left(n^2-l^2\right)}{c_l}T_l^n\left(x_k\right)T_n\left(x_j\right), \tag{33}$$

Also, $T_n\left(x_j\right)$ is the Chebyshev polynomial and coefficients $\gamma_j$ and $c_l$ are defined as:

$$\gamma_j=\begin{cases}\frac{1}{2} & j=0,\ or\ N\\ 1 & j=1,2,...N-1\end{cases}$$

(34a)

$$c_l = \begin{cases} 2 & l = 0, or\ N \\ 1 & l = 1, 2, \ldots N-1 \end{cases}$$

(34b)

### A. Procedure of methodology

A detailed procedure of the present method using CSCM is presented. We define the Chebyshev polynomials on the finite interval [-1, 1] and apply CSCM to make the suitable linear transformation. To achieve this, a transformation of the physical domain [-1, 1] to Chebyshev computational domain [-1, 1] is carried out. A sampling of the unknown function $w$ at the Chebyshev points to obtain the data vector $w = \left[w(x_0), w(x_1), w(x_2), \ldots\ldots w(x_N)\right]^T$ is performed. Next, we find the Chebyshev polynomial $P$ of degree $N$ that interpolates the data $\left(P(x_j) = w_j, \quad j = 0, 1, \ldots N\right)$ and obtain the spectral derivative vector $w$ by differentiating $P$ and evaluating it at the grid points. The outlined procedure transforms the nonlinear differential equation into nonlinear algebraic equations, which is solved by Newton's iterative method. Finally, a suitable transformation to map the physical domain [0, 1] to the computational domain [-1, 1] is then made to facilitate our computations.

Linear-law function

$$\frac{d^2\tilde{\theta}}{dX^2} + \beta X \frac{d^2\tilde{\theta}}{dX^2} + \beta \frac{d\tilde{\theta}}{dX} + 4Rd \frac{d^2\tilde{\theta}}{dX^2} - Ra\tilde{\theta}^2 - Nc^2\tilde{\theta} - Nr\tilde{\theta}^4 - 4NrC_T\tilde{\theta}^3 - 6NrC_T^2\tilde{\theta}^2 - 4NrC_T^3\tilde{\theta} = 0 \tag{35}$$

Power-law function

$$X^{-\beta}\frac{d^2\tilde{\theta}}{dX^2} - \beta X^{-\beta-1}\frac{d\tilde{\theta}}{dX} + 4Rd \frac{d^2\tilde{\theta}}{dX^2} - Ra\tilde{\theta}^2 - Nc^2\tilde{\theta} - Nr\tilde{\theta}^4 - 4NrC_T\tilde{\theta}^3 - 6NrC_T^2\tilde{\theta}^2 - 4NrC_T^3\tilde{\theta} = 0 \tag{36}$$

and the boundary conditions are

$$\tilde{\theta}'(-1) = 0, \quad \tilde{\theta}(1) = 1 \tag{37}$$

As explained in Section III (a), we transform Eq. (35) and (36) and the boundary condition to a group of nonlinear algebraic equations expressed as:

Linear-law function

$$\sum_{j=0}^{N} d_{kj}^2\tilde{\theta}(X_j) + \beta\sum_{j=0}^{N} d_{kj}^2\tilde{\theta}(X_j) + \beta\sum_{j=0}^{N} d_{kj}^1\tilde{\theta}(x_j) + 4Rd\sum_{j=0}^{N} d_{kj}^2\tilde{\theta}(X_j) - Ra\tilde{\theta}^2(x_j) - Nc^2\tilde{\theta}(x_j) - Nr\left[\tilde{\theta}(x_j)\right]^4 - 4NrC_T\left[\tilde{\theta}(x_j)\right]^3 - 6NrC_T^2\left[\tilde{\theta}(x_j)\right]^2 - 4NrC_T^3\tilde{\theta}(x_j) = 0 \tag{38}$$

Power-law function

$$\sum_{j=0}^{N}(X_j)^{-\beta} d_{kj}^2\tilde{\theta}(X_j) - \beta\sum_{j=0}^{N}(X_j)^{-\beta-1} d_{kj}^2\tilde{\theta}(x_j) + 4Rd\sum_{J=0}^{N} d_{kj}^2\tilde{\theta}(X_j) - Ra\tilde{\theta}^2(x_j) - Nc^2\tilde{\theta}(x_j) - Nr\left[\tilde{\theta}(x_j)\right]^4 - 4NrC_T\left[\tilde{\theta}(x_j)\right]^3 - 6NrC_T\left[\tilde{\theta}(x_j)\right]^2 - 4NrC_T^3\tilde{\theta}(x_j) = 0 \tag{39}$$

the boundary conditions are

$$\sum_{j=0}^{N} d_{kj}^1\tilde{\theta}(x_j) = 0, \quad \tilde{\theta}(x_j) = 1 \tag{40}$$

The above system of nonlinear algebraic equations is solved using Newton's iterative method to determine the temperature distribution of the porous fin with FGM.

It is noteworthy that for homogenous porous fin, $\beta = 0$. Therefore, the convergence criterion of the numerical solution along with error estimation is been set to

$$\sum_{i}^{N}\left|\tilde{\theta}_i^i - \tilde{\theta}^{i-1}\right| \le 10^{-4} \tag{41}$$

where $i$ is the number of iteration.

### B. Fin Efficiency

Fin efficiency is expressed as the ratio of effective rate of heat dissipated to the rate of heat that would dissipate if the entire fin is at base temperature. However, the total instantaneous surface heat loss is the sum of convective and radiative losses, which could be expressed as:

$$Q_{actual} = \int_0^L \left[hP(1-\varphi)(T - T_\infty) + \sigma\varepsilon P(T^4 - T_s^4)\right]dx \tag{42}$$

and an ideal heat transfer is the heat transfer from the fin when the entire fin surface is at base temperature, which could be expressed as:

$$Q_{ideal} = hPL(1-\varphi)(T_b - T_\infty) + \sigma\varepsilon PL(T_b^4 - T_s^4) \tag{43}$$

Therefore, the fin efficiency is expressed as:

$$\eta = \frac{Q_{actual}}{Q_{ideal}} = \frac{\int_0^L [Ph(1-\varphi)(T - T_\infty) + \sigma\varepsilon P(T^4 - T_s^4)]dx}{PhL(1-\varphi)(T_b - T_\infty) + \sigma\varepsilon PL(T_b^4 - T_s^4)} \tag{44}$$

## IV. RESULTS

The thermal models and the numerical solutions are simulated using MATLAB and the obtained results are presented in Fig. 3-10.

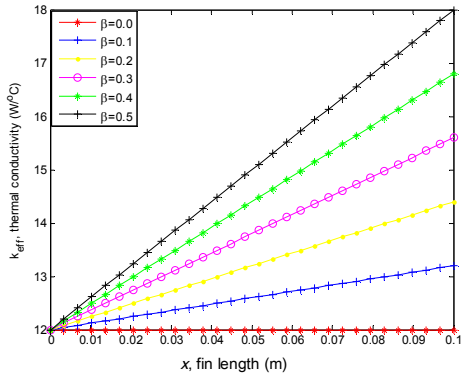


Fig. 3. Effect of in-homogeneity index on the linear- law effective thermal conductivity of the FGM fin

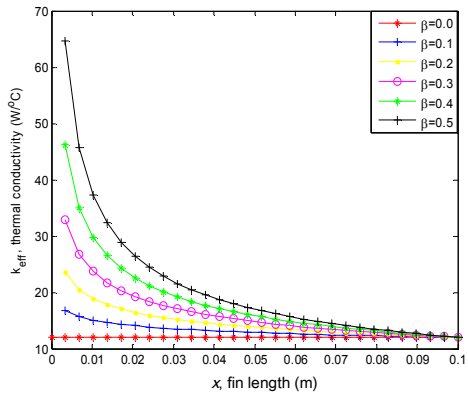


Fig. 4. Effect of in-homogeneity index on the power-law effective thermal conductivity of the FGM fin

Fig. 3 and 4 highlight the effects of the in-homogeneity index on the dimensional linear and power-law effective thermal conductivity of the fin of FGM. From Fig. 3 and 4, it can be seen that thermal conductivity increases with length in the linear-law function but decreases with length in the power-law function. The thermal behaviour shown in Fig 3 and 4 is as a result of the FGM, which is a new class of composite materials where the composition of macroscopic components generate continuous and smooth gradation of properties of the composite. Multiphase composites with continuously varying volume fractions are usually characterized by smoothly changing mechanical and thermal properties. The functionally graded fiber materials have dynamic, effective thermal properties and the volume fraction of the materials changes inversely. The non-homogeneous, variable microstructures of these materials cause continuously graded macroscopic properties including thermal conductivity, specific heat, mass density and elastic modulus. It should be stated that the effective thermal properties of FGM are dependent on the volume fraction of the constituent materials. Based on the composition of materials of the FGM, two common cases of thermal conductivities of FGM are presented in the present investigation. Therefore, the effective thermal conductivity of the fin increases with length in Fig. 3 but decreases with length in Fig. 4 since thermal conductivity is dependent on type, homogeneity, non-homogeneity and the volume fraction of the material composition of the FGM.

Figs. 5-8 highlight the effects of the in-homogeneity index on the temperature profile of the homogeneous material (HM) and FGM fin for varying thermogeometric parameters under the linear and power-law functions. Fig. 5 and 6 show the results of the linear-law function, whilst Fig 7 and 8 depicts the results of the power law function. From Fig. 5-8, it is shown that as the in-homogeneity index increases, the rate of heat transfer through the fin also increases. For all values of the convective and radiative parameter, the temperature gradient along the fin of FGM is less than HM fin for both linear and power-law functions. However, as the in-homogeneity index, $\beta$ increases, the temperature gradient decreases. This implies that the rate of heat transfer of the fin of FGM improves significantly as the value of the in-homogeneity index $\beta$ increases. These results show that the temperature profiles of the fin are highly sensitive in the power-law function for the FGM than that in the linear-law function. Also, FGM fin show significant improvement at low thermo-geometric convective and radiative parameters since the difference between HM fin and FGM fin profiles slightly decreases as the dimensionless thermogeometric parameters increases. The application of FGM decreases the thermal resistance along the fin, which is indicative that FGM fin exhibits higher temperature at the tip of the fin than HM fin. This shows that the rate of heat dissipation in the power-law FGM is significantly higher than in the linear class FGM. Furthermore, Figs. 5-8 illustrates the effects of conduction-convection *(Nc)*, conduction-radiation *(Nr)* and Rayleigh number *Ra* on the dimensionless temperature of the HM and FGM fin respectively. It is shown that the temperature profile of the fin increases as *Nc* and *Nr* increases. This is due to the fact that *Nc* and *Nr* are dependent on the coefficient of heat transfer, the emissivity of the fin material and thermal conductivity, all of which are function of the temperature variation between the fin and surrounding fluid. Therefore, as the differential temperature, *Nc* and *Nr* increases, the rate of heat transfer is enhanced in the fin. Additionally, it is shown that as *Ra* increases, temperature decreases rapidly whilst the rate of heat transfer through the fin increases.

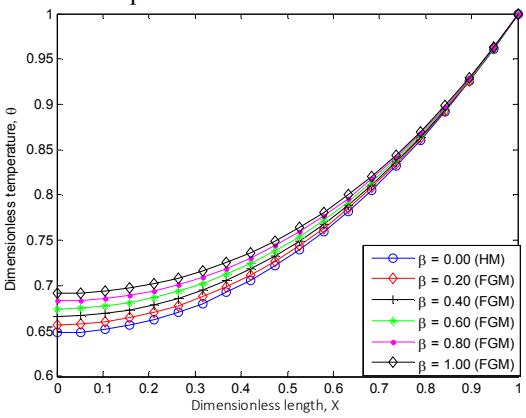


(a)

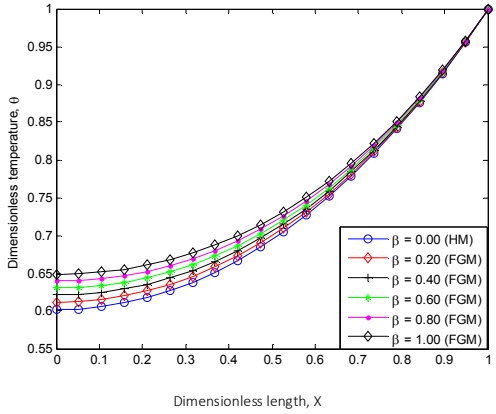


(b)

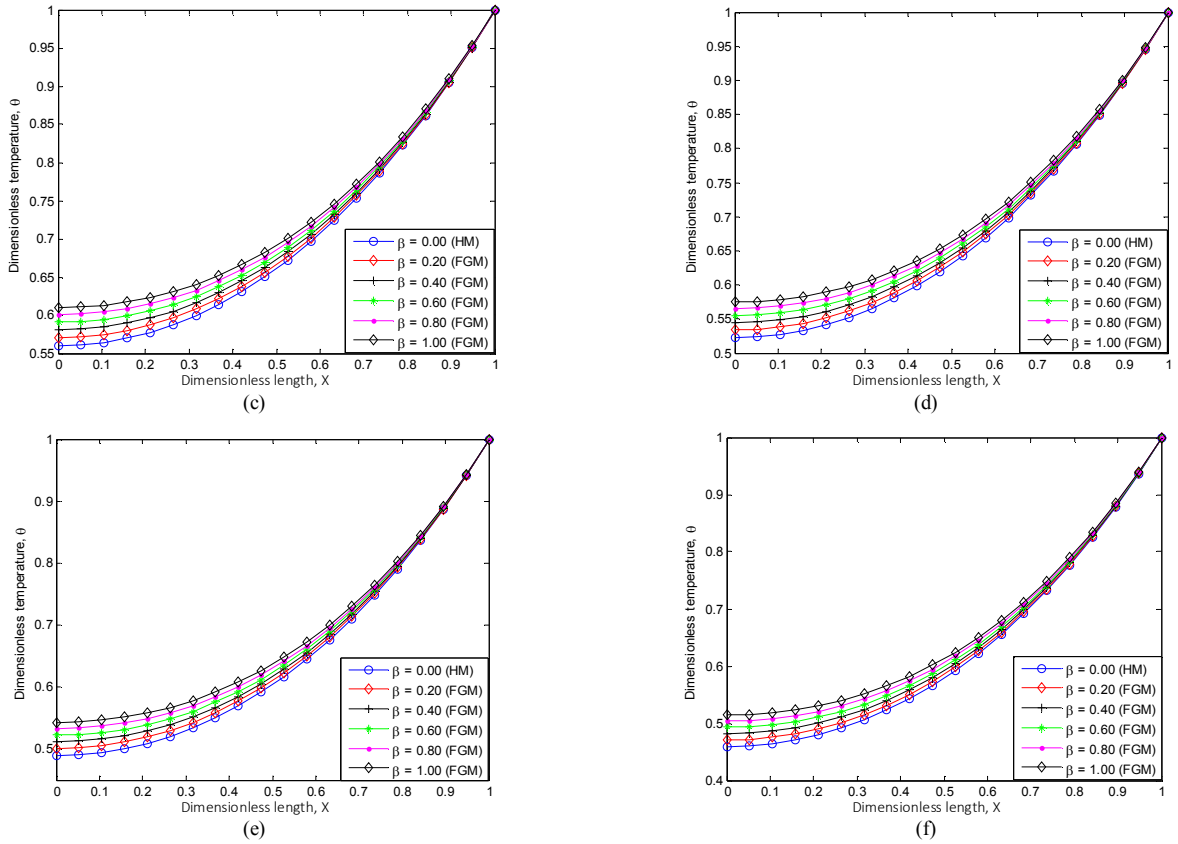


Fig. 5. Temperature profile of fin for different thermo-geometric parameters under linear-law function when (a) *Nr=0.0, Ra= 0.01, Nc =1.0* (b) *Nr=0.2, Ra=0.01, Nc=1.0,* (c) *Nr=0.1, Ra=0.01, Nc=1.0* (d) *Nr=0.1, Ra=0.01, Nc=1.2* (e) *Nr=0.1, Ra=0.01, Nc =1.5* (f) *Nr=0.2, Ra=0.01, Nc=1.*

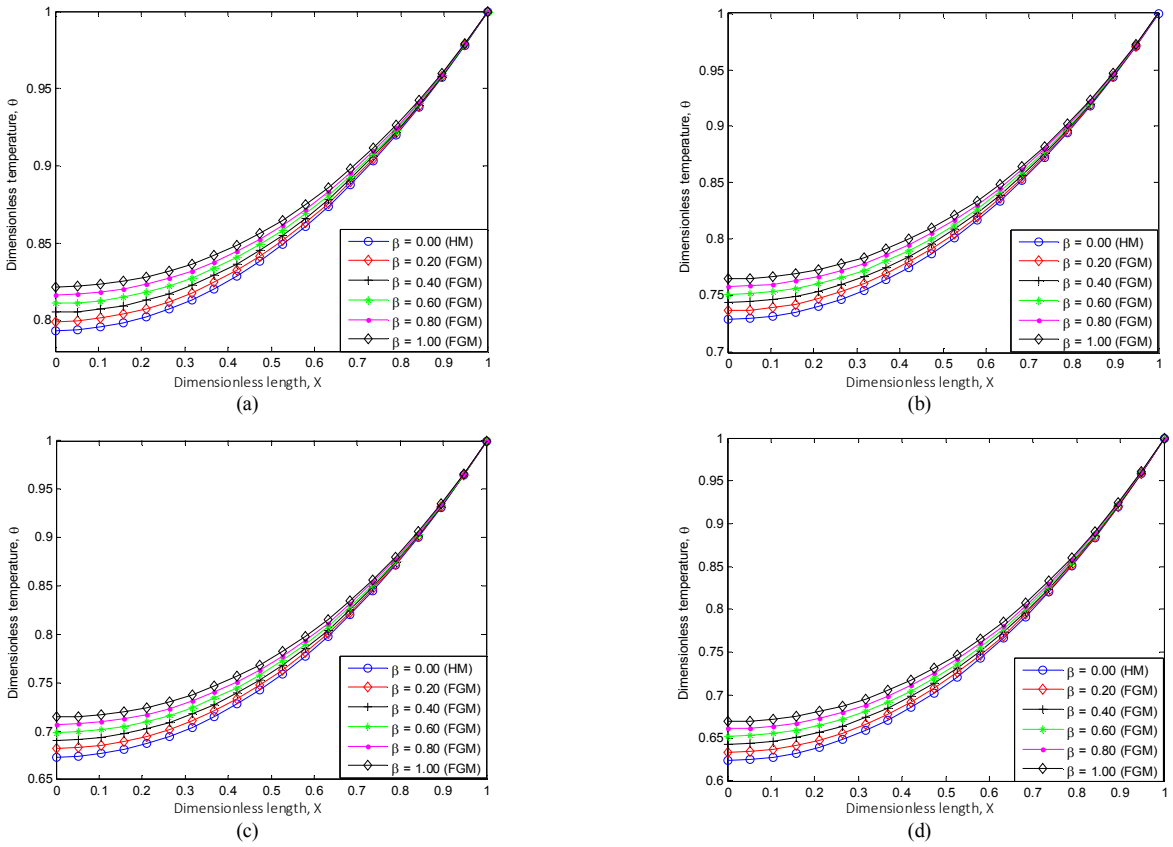

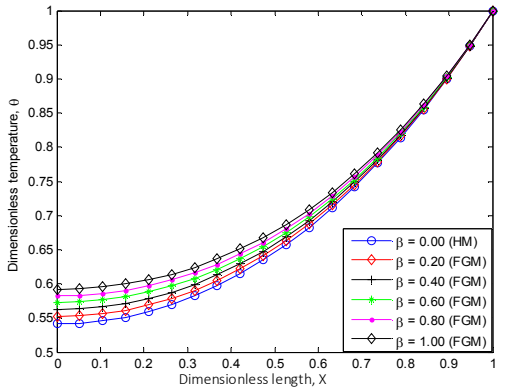


(e)

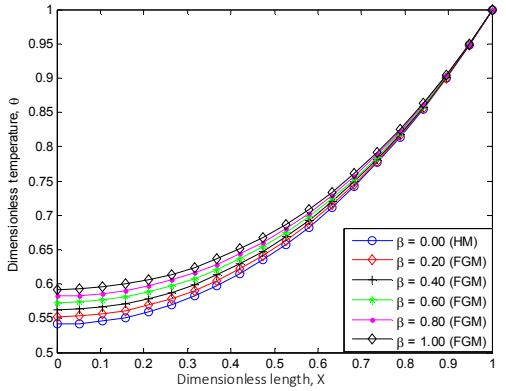


(f)

Fig. 6. Temperature profile of fin for varying thermo-geometric parameter under linear-law function when (a) *Nc=0.5, Ra= 0.01, Nr =0.0* (b) *Nc=0.1, Ra=0.01, Nr=0.2* (c) *Nc=0.1, Ra=0.01, Nr=0.4* (d) *Nc=0.2, Ra=0.01, Nr=0.3* (e) *Nc=0.5, Ra=0.01, Nr=0.2* (f) *Nc=0.2, Ra=0.01, Nr=1.0*

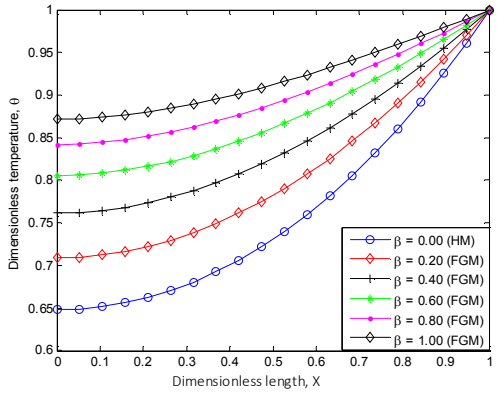


(a)

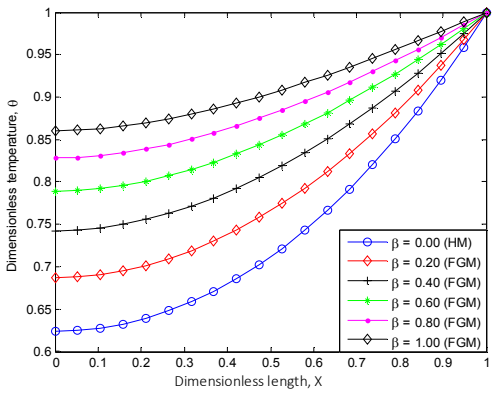


(b)

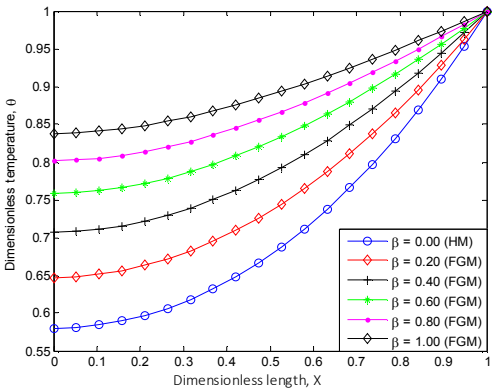


(c)

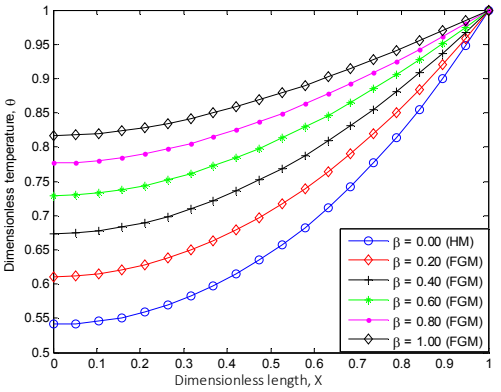


(d)

Fig. 7. Temperature profile of fin for different thermo-geometric parameter under power-law function when (a) *Nr*=0.0, Ra= 0.01, *Nc* =1.0 (b) *Nr*=0.1, *Ra*=0.01, *Nc*=0.5, (c) *Nr*=0.1, Ra=0.01, *Nc*=0.6 (d) *Nr*=0.2, *Ra*=0.01, *Nc*=0.5

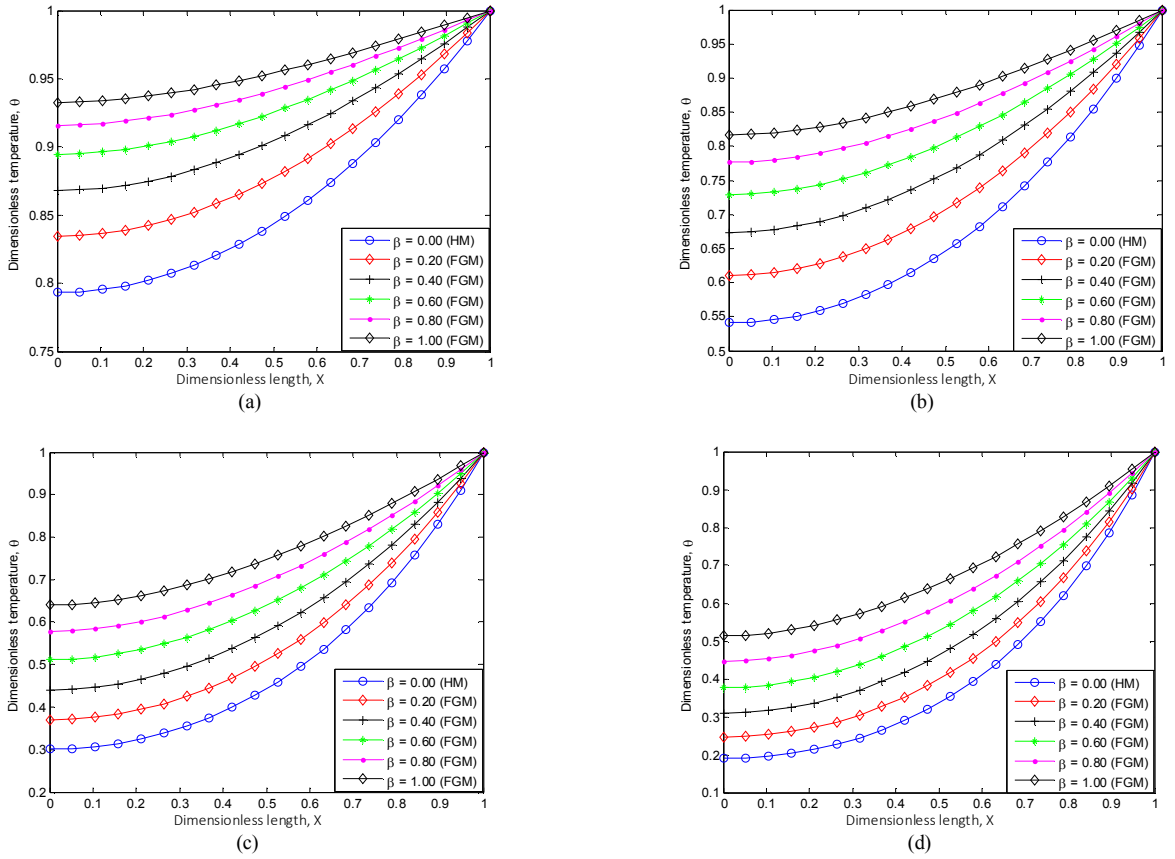


Fig. 8. Dimensionless temperature profile of fin at varying thermo-geometric parameters under power-law function when (a) *Nc*=0.0, Ra=0.01, *Nr*=0.5 (b) *Nc*=0.1, Ra=0.01, *Nr*=0.6 (c) *Nc*=1.0, Ra=0.01, *Nr*=0.1 (d) *Nc*=2.0, Ra=0.01, *Nr*=0.2

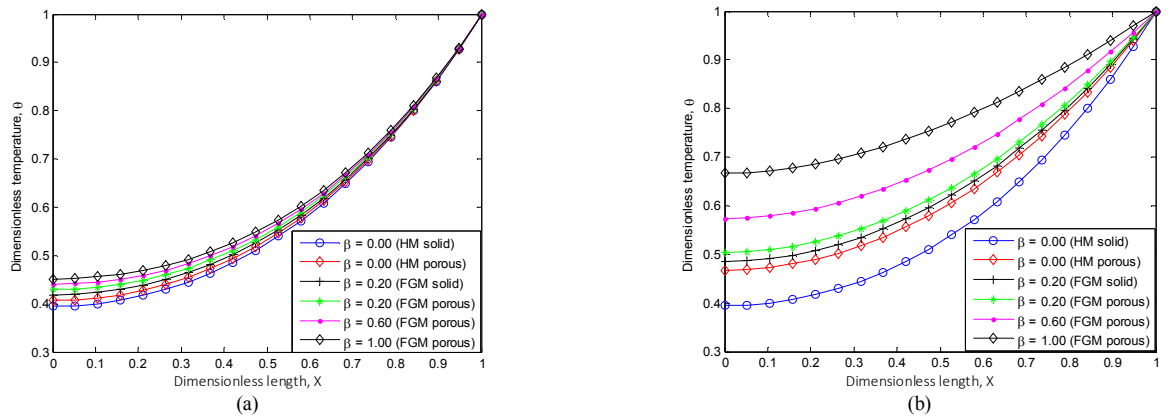


Fig. 9. Porosity effect on temperature profile of fin at varying thermo-geometric parameters as: (a) linear-law function *Nc*=3.0, *Ra*=0.02, *Nr*=0.6 (b) power-law function *Nc*=3.0, *Ra*=0.02, *Nr*=0.6

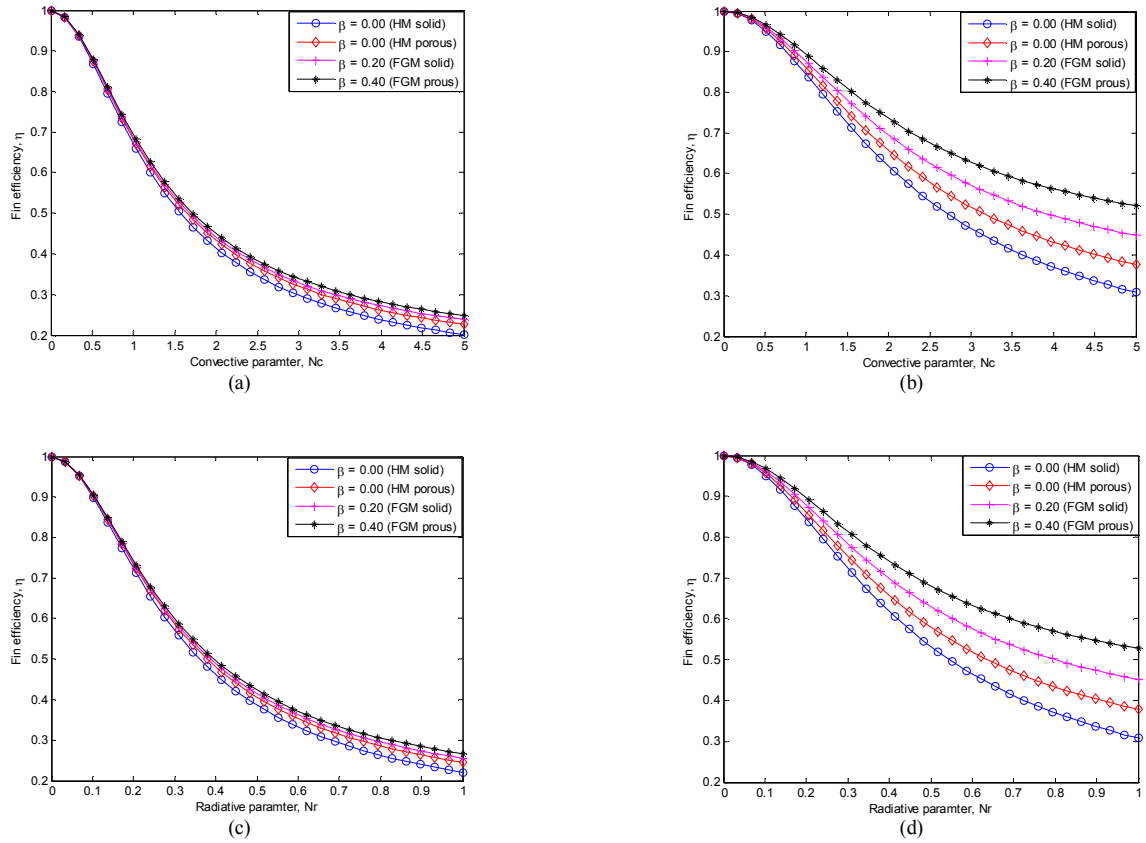


Fig. 10. Fin efficiency at varying thermo-geometric parameter (a) linear-law function when *Nc*=1.0, *Ra*= 0.01, *Nr* =0.1 (b) power-law function *Nc*=1.0, a=0.01, *Nr*=0.1 (c) linear-law function *Nc*=2.0, *Ra*=0.01, *Nr*=0.1 (d) power-law function *Nc*=2.0, Ra=0.01, *Nr*=0.1

As *Da* and *Ra* decrease the permeability parameter decreases which consequently increases the collision between the saturated fluid flow and the pores of the porous media, resulting in an increase in the fin temperature. Therefore, decrease in *Ra* increases the fin temperature. Therefore, a higher value of *Ra* enhances the rate of heat transfer between the fin and the air flow, which subsequently increase the rate of heat transfer through the fin.

Moreover, by comparing the thermal responses of the fin with the thermogeometric parameters *Nc, Nr* and *Ra* under the linear and power laws, the power law thermal model exhibits a more sensitive response to variations in the values of *Nc, Nr* and *Ra* as compared to linear law thermal model. This shows that there is an improved rate of heat transfer in the power law thermal model than the linear law thermal model. This fact is illustrated in the fin temperature profiles as shown in Fig. 5-8. The effects of porosity on the temperature distribution of the fin under the linear and power law thermal model are presented in Fig. 9. From Fig 9, it can be seen that as the porosity parameter increases, the fin temperature decreases rapidly and the rate of heat transfer through the fin increases. The rapid decrease in the fin temperature with increase in the porosity parameter occurs as a result of several combining factors including (*i*) increase in the porosity parameter increases the permeability of the porous fin which subsequently increases the ability of the porous fluid to penetrate through the fin pores, (*ii*) The effect of buoyancy force increases the convective mechanism of the fin (*iii*) The rate of heat flow is enhanced via the convective mechanism improves the thermal performance of the fin. Therefore, the porosity parameter improves the thermal efficiency of the fin due to increase in convected heat transfer.

The effect of *Nc*, *Nr* and *Ra* on the thermal efficiency of the fin for the linear and power law is presented in Fig. 10. The power-law model responds more thermally than in the linear law. It can be seen in both cases that the thermal efficiency of the fin improves as the values of the *Nc, Nr* and *Ra* increases. It is interesting to state that the thermal efficiency of the porous FGM fin is higher than the solid FGM fin. The improved efficiency of the porous FGM fin is enhanced by increase in the porosity or permeability parameter. This is because as *Ra*, the effect of buoyancy force increases, resulting in increased heat dissipation via convection.

The improvement in the energy saving capability of FGM heat sinks in both linear and power-law class plays a fundamental role in the field of electronics. A practical implication will be miniaturized fan size which would result in reduced airflow rate within sensitive devices and controlling the acoustic level, resulting in lower distortion, and consequently increased lifespan of various consumer and high power electronics.

Table I. Comparison of temperature results

| Variable $X$ | Runge-Kutta – Shooting Method (RKSM) | Homotopy Analysis Method (HAM) [39] | CSCM (Present Study) | % Error \|RKSM-HAM\| | % Error \|RKSM-CSCM\| |
|---|---|---|---|---|---|
| 0.00 | 0.863499231 | 0.863499664 | 0.863499158 | 0.000000433 | 0.000000073 |
| 0.05 | 0.863828568 | 0.863829046 | 0.863828540 | 0.000000478 | 0.000000028 |
| 0.10 | 0.864817090 | 0.864817539 | 0.864817031 | 0.000000449 | 0.000000059 |
| 0.15 | 0.866465743 | 0.866466182 | 0.866465671 | 0.000000439 | 0.000000072 |
| 0.20 | 0.868776261 | 0.868776709 | 0.868776195 | 0.000000448 | 0.000000066 |
| 0.25 | 0.871751104 | 0.871751555 | 0.871751037 | 0.000000451 | 0.000000067 |
| 0.30 | 0.875393404 | 0.875393859 | 0.875393336 | 0.000000455 | 0.000000068 |
| 0.35 | 0.879707010 | 0.879707472 | 0.879706946 | 0.000000462 | 0.000000064 |
| 0.40 | 0.884656900 | 0.884696967 | 0.884696438 | 0.000000467 | 0.000000062 |
| 0.45 | 0.890367181 | 0.890367650 | 0.890367120 | 0.000000469 | 0.000000061 |
| 0.50 | 0.896725096 | 0.896725569 | 0.896725040 | 0.000000473 | 0.000000056 |
| 0.55 | 0.903777060 | 0.903777531 | 0.903777007 | 0.000000471 | 0.000000053 |
| 0.60 | 0.911530658 | 0.911531120 | 0.911530606 | 0.000000462 | 0.000000052 |
| 0.65 | 0.919994259 | 0.919994710 | 0.919994212 | 0.000000451 | 0.000000047 |
| 0.70 | 0.929177056 | 0.929177488 | 0.929177015 | 0.000000432 | 0.000000041 |
| 0.75 | 0.939089079 | 0.939089476 | 0.939089039 | 0.000000397 | 0.000000040 |
| 0.80 | 0.949741203 | 0.949741555 | 0.949741166 | 0.000000352 | 0.000000037 |
| 0.85 | 0.961145189 | 0.961145491 | 0.961145166 | 0.000000302 | 0.000000023 |
| 0.90 | 0.973313764 | 0.973313964 | 0.973313722 | 0.000000200 | 0.000000042 |
| 0.95 | 0.986260549 | 0.986260599 | 0.985260463 | 0.000000005 | 0.000000086 |
| 1.00 | 1.000000000 | 1.000000000 | 1.000000000 | 0.000000000 | 0.000000000 |

Table I highlights the comparative results of the present study, numerical method using 4th order Runge-Kutta with shooting method (RKSM) and an approximate analytical method using homotopy analysis method (HAM) [39]. The percentage errors of the various methods are also presented. Table I proves that the result of the present work using CSCM is highly accurate and is in excellent agreement with the result of the RKSM and HAM. From Table I, it is also shown that there is congruence between the RKSM and CSCM solutions for a higher order of accuracy, as the result of CSCM have a smaller marginal difference with RKSM as compared to HAM. It can also be seen that CSCM agrees more with the results of RKSM than HAM.

Furthermore, the results from Table I show that the rate of convergence, when $N$ is even (for all positive integer in the CSCM iterative scheme) is faster than when $N$ is odd. Moreover, the processing time of CSCM increases as $N$ increases for the computational simulations performed in the present work. The average computational time to generate the results of the present work is 0.026192 sec.

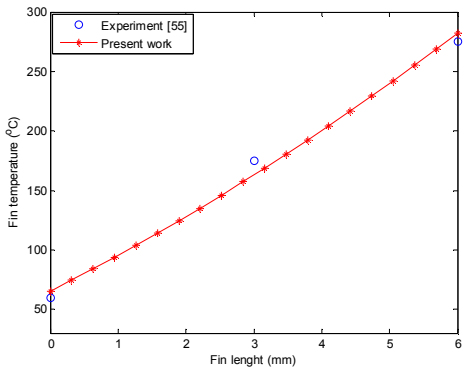


Fig. 11. Comparison of experimental and model results

This establishes that CSCM is a computationally reliable for solving the nonlinear heat transfer problem necessary for thermal management of various consumer and high-power electronics. Nonetheless, it is worth stating that there are no available experimental results for the validation of fin of FGM. However, there is the possibility of comparison at the level of HM. Therefore, in Fig. 11, the present model results based on fin of HM is compared with established experimental results [40]. From Fig. 11, we show that good agreement is established between the experimental results and our present work.

## V. Conclusion

In this paper, we present a numerical thermal analysis of a porous fin of functionally graded material for improved cooling of consumer electronics with linear and power-law functions. The developed thermal models are solved using Chebyshev spectral collocation method. The effects of thermogeometric parameters as well as the inhomogeneous index on the performance of the FGM porous fin are investigated. The results from the analysis show that increase in the inhomogeneity index of FGM, convective and radiative parameters improve the thermal efficiency of the porous fin heatsink. Parametric study shows that for all values of *Nc, Rd*, the temperature gradient along the fin of FGM is negligible compared with the fin of HM for both linear and power-law functions. The present method, exhibit increased accuracy over compared numerical and approximate analytical methods. The present investigation helps to understand the thermal response of porous fin of FGM under various operating conditions. Finally, the findings of the investigation are of practical implication in the design of thermally-enhanced,

miniaturized heatsinks of FGM for improved cooling of various consumer electronics.

## ACKNOWLEDGMENT

This work is supported in part from PhD sponsorship of the first author by the Tertiary Education Trust Fund of the Federal Government of Nigeria.

## REFERENCES

[1] G. E. Moore, "Cramming more components onto integrated circuits, Reprinted from Electronics, volume 38, number 8, April 19, 1965, pp.114 ff," *IEEE Solid-State Circuits Society Newsletter,* vol. 11, pp. 33-35, 2006.

[2] R. Mahajan, C. Chia-pin, and G. Chrysler, "Cooling a Microprocessor Chip," *Proceedings of the IEEE,* vol. 94, pp. 1476-1486, 2006.

[3] Wikipedia. (2017). *Heat sink/computer*. Available: https://en.wikipedia.org/wiki/Heat_sink

[4] S. Kiwan and M. A. Al-Nimr, "Using Porous Fins for Heat Transfer Enhancement," *Journal of Heat Transfer,* vol. 123, pp. 790-795, 2000.

[5] A. Shalchi-Tabrizi and H. R. Seyf, "Analysis of entropy generation and convective heat transfer of Al2O3 nanofluid flow in a tangential micro heat sink," *International Journal of Heat and Mass Transfer,* vol. 55, pp. 4366-4375, 2012.

[6] S. M. H. Hashemi, S. A. Fazeli, H. Zirakzadeh, and M. Ashjaee, "Study of heat transfer enhancement in a nanofluid-cooled miniature heat sink," *International Communications in Heat and Mass Transfer,* vol. 39, pp. 877-884, 2012.

[7] T.-C. Hung, W.-M. Yan, X.-D. Wang, and C.-Y. Chang, "Heat transfer enhancement in microchannel heat sinks using nanofluids," *International Journal of Heat and Mass Transfer,* vol. 55, pp. 2559-2570, 2012.

[8] H. R. Seyf and M. Feizbakhshi, "Computational analysis of nanofluid effects on convective heat transfer enhancement of micro-pin-fin heat sinks," *International Journal of Thermal Sciences,* vol. 58, pp. 168-179, 2012.

[9] G. A. Oguntala and R. A. Abd-Alhameed, "Haar Wavelet Collocation Method for Thermal Analysis of Porous Fin with Temperature-dependent Thermal Conductivity and Internal Heat Generation," *Journal of Applied and Computational Mechanics,* vol. 3, pp. 185-191, 2017.

[10] G. Oguntala, R. Abd-Alhameed, G. Sobamowo, and H.-S. Abdullahi, "Improved thermal management of computer microprocessors using cylindrical-coordinate micro-fin heat sink with artificial surface roughness," *Engineering Science and Technology, an International Journal,* 2018/06/19/ 2018.

[11] S. A. Fazeli, S. M. Hosseini Hashemi, H. Zirakzadeh, and M. Ashjaee, "Experimental and numerical investigation of heat transfer in a miniature heat sink utilizing silica nanofluid," *Superlattices and Microstructures,* vol. 51, pp. 247-264, 2012.

[12] M. Faraji and H. E. Qarnia, "Numerical Study of Free Convection Dominated Melting in an Isolated Cavity Heated by Three Protruding Electronic Components," *IEEE Transactions on Components and Packaging Technologies,* vol. 33, pp. 167-177, 2010.

[13] J. Ma, Y. Sun, and B. Li, "Spectral collocation method for transient thermal analysis of coupled conductive, convective and radiative heat transfer in the moving plate with temperature dependent properties and heat generation," *International Journal of Heat and Mass Transfer,* vol. 114, pp. 469-482, 2017.

[14] G. Oguntala, G. Sobamowo, R. Abd-Alhameed, and S. Jones, "Efficient Iterative Method for Investigation of Convective–Radiative Porous Fin with Internal Heat Generation Under a Uniform Magnetic Field," *International Journal of Applied and Computational Mathematics,* vol. 5, p. 13, 2019.

[15] J. L. Gess, S. H. Bhavnani, and R. W. Johnson, "Experimental Investigation of a Direct Liquid Immersion Cooled Prototype for High-Performance Electronic Systems," *IEEE Transactions on Components, Packaging and Manufacturing Technology,* vol. 5, pp. 1451-1464, 2015.

[16] R. S. Kumar and S. Jayavel, "Forced Convective Air-Cooling Effect on Electronic Components of Different Geometries and Orientations at Flow Shedding Region," *IEEE Transactions on Components, Packaging and Manufacturing Technology,* vol. 8, pp. 597-605, 2018.

[17] R. Leena, R. V. Renjith, and M. J. Prakash, "Experimental and Numerical Investigations on Steady and Unsteady Jet Impingement Cooling for High-Power Electronics," *IEEE Transactions on Components, Packaging and Manufacturing Technology,* vol. 5, pp. 636-640, 2015.

[18] G. A. Oguntala, G. M. Sobamowo, N. N. Eya, and R. A. Abd-Alhameed, "Investigation of Simultaneous Effects of Surface Roughness, Porosity, and Magnetic Field of Rough Porous Microfin Under a Convective–Radiative Heat Transfer for Improved Microprocessor Cooling of Consumer Electronics," *IEEE Transactions on Components, Packaging and Manufacturing Technology,* vol. 9, pp. 235-246, 2019.

[19] R. Chiba, "Stochastic thermal stresses in an FGM annular disc of variable thickness with spatially random heat transfer coefficients," *Meccanica,* vol. 44, pp. 159-176, April 01 2009.

[20] H.-L. Lee, W.-J. Chang, W.-L. Chen, and Y.-C. Yang, "Inverse heat transfer analysis of a functionally graded fin to estimate time-dependent base heat flux and temperature distributions," *Energy Conversion and Management,* vol. 57, pp. 1-7, 2012.

[21] R. Srikanth, P. Nemani, and C. Balaji, "Multi-objective geometric optimization of a PCM based matrix type composite heat sink," *Applied Energy,* vol. 156, pp. 703-714, 2015.

[22] R. Srikanth and C. Balaji, "Experimental investigation on the heat transfer performance of a PCM based pin fin heat sink with discrete heating," *International Journal of Thermal Sciences,* vol. 111, pp. 188-203, 2017.

[23] R. Srikanth and C. Balaji, "Heat Transfer Correlations for a Composite PCM Based 72 Pin Fin Heat Sink with Discrete Heating at the Base," *INAE Letters,* vol. 2, pp. 65-71, 2017.

[24] S. A. O. David Gottlieb, *Numerical Analysis of Spectral Methods: Theory and Applications (CBMS-NSF Regional Conference Series in Applied Mathematics*: Society for Industrial and Applied Mathematics, 1987.

[25] Y. H. Claudio Canuto, Alfio Quarteroni, Thomas A. Zang, *Spectral Methods in Fluid Dynamics*: Springer Berlin Heidelberg, 1988.

[26] J. P. Wang, "Fundamental problems in spectral methods and finite spectral method," *Acta Aerodynamica Sinica,* vol. 19, pp. 161-171, 2001.

[27] N. T. Eldabe and M. E. M. Ouaf, "Chebyshev finite difference method for heat and mass transfer in a hydromagnetic flow of a micropolar fluid past a stretching surface with Ohmic heating and viscous dissipation," *Applied Mathematics and Computation,* vol. 177, pp. 561-571, 2006.

[28] E. H. Doha, A. H. Bhrawy, and S. S. Ezz-Eldien, "Efficient Chebyshev spectral methods for solving multi-term fractional orders differential equations," *Applied Mathematical Modelling,* vol. 35, pp. 5662-5672, 2011.

[29] A. Aziz and M. M. Rahman, "Thermal Performance of a Functionally Graded Radial Fin," *International Journal of Thermophysics,* vol. 30, p. 1637, July 30 2009.

[30] R. Hassanzadeh and M. Bilgili, "Assessment of Thermal Performance of Functionally Graded Materials in Longitudinal Fins," *Journal of Engineering Physics and Thermophysics,* vol. 91, pp. 79-88, January 01 2018.

[31] M. Shahbabaei and S. Saedodin, "Thermal Performance of Convective-Radiative Heat Transfer in Porous Fins," *Walailak Journal of Science and Technology,* vol. 11, pp. 1105-1117, 2013.

[32] C. Bardos, F. Golse, and B. Perthame, "The Rosseland approximation for a simplified model of the radiative transfer equations," *Comptes Rendus des Seances de l'Academie des Sciences Serie 1,* vol. 301, pp. 627-630, 1985.

[33] H. Kumar and G. Nagarajan, "A Bayesian inference approach: estimation of heat flux from fin for perturbed temperature data," *Sādhanā,* vol. 43, p. 62, April 16 2018.

[34] K. D. Cole, C. Tarawneh, and B. Wilson, "Analysis of flux-based fins for estimation of heat transfer coefficient," *International Journal of Heat and Mass Transfer,* vol. 52, pp. 92-99, 2009.

[35] J. Mao and S. Rooke, "Transient analysis of extended surfaces with convective tip," *International Communications in Heat and Mass Transfer,* vol. 21, pp. 85-94, 1994.
[36] N. V. Suryanarayana, "Transient Response of Straight Fins," *Journal of Heat Transfer (Part II),* vol. 97, pp. 417-423, 1976.
[37] B. Kundu and K.-S. Lee, "Analytical tools for calculating the maximum heat transfer of annular stepped fins with internal heat generation and radiation effects," *Energy,* vol. 76, pp. 733-748, 2014.
[38] S. Kiwan, "Effect of radiative losses on the heat transfer from porous fins," *International Journal of Thermal Sciences,* vol. 46, pp. 1046-1055, 2007.
[39] S. Rezazadeh Amirkolaei, Ganji, DD, Salarian, H, "Determination Of Temperature Distribution For Porous Fin Which Is Exposed To Uniform Magnetic Field To A Vertical Isothermal Surface By Homotopy Analysis Method And Collocation Method," *Indian Journal of Scientific Research,* vol. 1, pp. 215-222, 2014.
[40] A. K. Subodh Kr. Sharma, Pratibha Kumari, "Experimental Investigation of temperature in Fins," *International Journal of Applied Engineering Research,* vol. 13, pp. 354-357, 2018.

**George A. Oguntala** (*M'13*) received the B.Sc. degree in Electronic and Computer Engineering, M.Sc. in Systems Engineering with an option in Engineering Analysis and an MBA in Human Resources Management. He is currently pursuing the PhD degree in Electrical Engineering at the University of Bradford, UK.
Mr Oguntala is a Chartered Engineer and a member of the Institution of Engineering and Technology, Association of Computing Machinery, International Association of Engineers, Nigerian Institution of Electrical Electronics Engineers, Nigeria Society of Engineers and the Engineering Council. He is also an Associate member of the Higher Education Academy. His current research interest includes thermal management and microprocessor cooling, applied mathematics, Smart health and Smart Home, antenna, propagation and RFID.

**Gbeminiyi M. Sobamowo** received the B.Sc., M.Sc. and PhD degree all in mechanical engineering from University of Lagos, Akoka, Lagos, Nigeria, in 2013.
He is currently a Lecturer with the Mechanical Engineering Department, University of Lagos. His research interests include energy systems modelling, simulation and design, renewable energy systems, flow and heat transfer and thermal fluidic induced instability in energy systems. He is a member of the
Nigerian Institution of Mechanical Engineers, Nigeria Society of Engineers, and the Engineering Council.

**Raed A. Abd-Alhameed** (M'02–SM'13) received the B.Sc. and M.Sc. degrees from Basrah University, Basrah, Iraq, in 1982 and 1985, respectively, and the Ph.D. degree from the University of Bradford, West Yorkshire, U.K., in 1997, all in electrical engineering, where he is currently a Professor of electromagnetic and radio-frequency engineering. He has been a Research Visitor with Wrexham University, U.K., since 2009, covering the wireless and communications research areas. He is the Leader of Radio Frequency, Propagation, Sensor Design and Signal Processing Research Group; in addition to leading the Communications Research Group for years within the School of Engineering and Informatics, Bradford University. He has long years' research experience in the areas of radio frequency, signal processing, propagations, antennas, and electromagnetic computational techniques, and has published over 500 academic journal and conference papers; in addition, he has co-authored four books and several book chapters. His interests include 5G green communications systems, computational methods and optimizations, wireless and mobile communications, sensor design, EMC, MIMO systems, beam steering antennas, energy-efficient PAs, and RF predistorter design applications. He is a Principal Investigator for several funded applications to EPSRCs and a Leader of several successful knowledge transfer programs such as with Arris (previously known as Pace plc), Yorkshire Water plc, Harvard Engineering plc, IETG Ltd., Seven Technologies Group, Emkay Ltd., and Two World Ltd. He has also been a Co-Investigator in several funded research projects, including H2020 MARIE Skłodowska-CURIE ACTIONS: Innovative Training Networks ''Secure Network Coding for Next Generation Mobile Small Cells 5G-US,'' Nonlinear and demodulation mechanisms in biological tissue (Department of Health, Mobile Telecommunications and Health Research Programme), and Assessment of the Potential Direct Effects of Cellular Phones on the Nervous System (EU: collaboration with six other major research organizations across Europe). He received the Business Innovation Award for his successful KTP with Pace and Datong companies on the design and implementation of MIMO sensor systems and antenna array design for service localizations. He is the Chair of several successful workshops on Energy Efficient and Reconfigurable Transceivers: Approach towards Energy Conservation and CO2 Reduction that addresses the biggest challenges for future wireless systems. He was appointed as a Guest Editor of the IET Science, Measurements and Technology Journal, from 2009 to 2012. He is the Fellow of the Institution of Engineering and Technology, a Fellow of the Higher Education Academy and a Chartered Engineer.

**James M. Noras** received the B.Sc. degree in physics from St. Andrews University, Scotland, in 1973, the M.Sc. degree in mathematics from Open University, U.K., in 1995, and the PhD degree in semiconductor physics from St. Andrews University in 1978. He is currently a Senior Lecturer with the School of Engineering and Informatics, University of Bradford, U.K. He is also the Director of three internationally franchised B.Eng. courses in electrical and electronic engineering. He has published 59 journals and 93 conference papers, in fundamental semiconductor physics, analogue and digital circuit design, digital signal processing, and RF system design and evaluation. His main research interests are now in digital system design and implementation, DSP and coding for communication systems, and localization algorithms for mobile systems. He is a member of the Institute of Physics and a Chartered Physicist.